

Electrical transport properties of highly doped $\text{PrBa}_{2-x}\text{Sr}_x\text{Cu}_3\text{O}_7$ thin films prepared by pulsed laser deposition

Y. G. Zhao,* Z. W. Dong,† M. Rajeswari, R. P. Sharma, and T. Venkatesan

Center for Superconductivity Research, Department of Physics, University of Maryland, College Park, Maryland 20742

(Received 23 January 1998)

We have prepared single phase $\text{PrBa}_{2-x}\text{Sr}_x\text{Cu}_3\text{O}_7$ ($x=0,1.3,1.6$) thin films with dopant concentration exceeding the solid solubility limit by using the pulsed laser deposition method. The resistivity of the doped thin films decreases with increasing dopant concentration. For $x=1.3$, the electrical resistivity ratios $\rho(4.2\text{ K})/\rho(300\text{ K})=2.56$; while for $x=1.6$, $\rho(4.2\text{ K})/\rho(300\text{ K})=1.98$, comparable to that of the $\text{Y}_{0.5}\text{Pr}_{0.5}\text{Ba}_2\text{Cu}_3\text{O}_7$ sample, which is very close to the insulator-metal transition. Moreover, the resistivity of the $\text{PrBa}_{0.4}\text{Sr}_{1.6}\text{Cu}_3\text{O}_7$ thin film is very close to the Ioffe-Regel limit, also indicating its proximity to the insulator-metal transition. The decrease of the resistivity with doping for $\text{PrBa}_{2-x}\text{Sr}_x\text{Cu}_3\text{O}_7$ can be explained by the decrease of the hybridization between Pr $4f$ and O $2p$ states in the CuO_2 planes due to the Sr doping induced increase of the Pr-O bond length. [S0163-1829(98)01025-X]

INTRODUCTION

It is well known that all $R\text{Ba}_2\text{Cu}_3\text{O}_7$ (R =rare-earth elements) materials, except $R=\text{Pr,Ce}$, are superconductors with T_c above 90 K. The absence of superconductivity in this $\text{PrBa}_2\text{Cu}_3\text{O}_7$ (PBCO) compound is not fully understood, although a lot of work has been done concerning this issue.¹ Recently, there has been a paper stating that PBCO is a superconductor.² There is a need for further research to understand the anomalous properties of PBCO. The electrical transport property of PBCO shows variable range hopping (VRH) behavior^{3,4} and the Pr ions order antiferromagnetically at 17 K, which is an order of magnitude higher than the Néel temperature of other $R\text{Ba}_2\text{Cu}_3\text{O}_7$ compounds.^{5,6} Currently, several models have been proposed,¹ such as hole filling, hybridization of the Pr $4f$ and O $2p$ states of the CuO_2 plane, magnetic pair breaking, and mixed valency, etc., to interpret the anomalous properties of PBCO. It seems that the hybridization model is essential for the explanation of the anomalous properties of PBCO. In this scenario, the Pr $4f$ state hybridizes with the O $2p$ state, leading to the localization of the carriers (holes) and thus destroys superconductivity.⁷⁻¹⁵

In a previous work involving bulk materials,¹⁶ we have shown that Sr doping at a Ba site in PBCO increases the distance between the Pr and O ions in the CuO_2 planes, resulting in the decrease of the hybridization between the Pr $4f$ and the O $2p$ states in the CuO_2 plane. A dramatic decrease of resistivity occurred for the doped samples. However, it was also found that the solid solubility limit of Sr in PBCO is about 0.8, which hindered further doping.

Pulsed laser deposition (PLD) has played a very important role in the fabrication of a variety of thin films. It has also proved to be very effective in growing highly doped thin films whose dopant concentration cannot be achieved by the solid-state reaction method.^{17,18} In this paper, we report the fabrication and characterization of pure phase $\text{PrBa}_{2-x}\text{Sr}_x\text{Cu}_3\text{O}_7$ thin films with $x=0,1.3,1.6$ prepared by PLD. The resistivity of the doped thin films decreases with

doping and this is consistent with the results of bulk materials, which can be explained by a decrease of the hybridization between the Pr $4f$ and O $2p$ states induced by Sr doping.

EXPERIMENT

The thin films were deposited from high-purity, high-density PBCO, $\text{PrBa}_{0.7}\text{Sr}_{1.3}\text{Cu}_3\text{O}_7$, and $\text{PrBa}_{0.4}\text{Sr}_{1.6}\text{Cu}_3\text{O}_7$ targets on (001) LaAlO_3 (LAO) substrates by PLD with a KrF laser ($\lambda=248\text{ nm}$). Several laser energy fluences, substrate temperatures, and oxygen ambient pressures during deposition were used to optimize the necessary conditions for the film growth. After deposition, the films were cooled in about 500 Torr oxygen and kept at 460 °C for 1 h before cooling down to room temperature. The thickness of the film was about 200 nm as measured with a Dektak α -step profilometer. A Rigaku x-ray diffractometer (XRD) with Cu $K\alpha$ radiation was used for phase and crystallinity analysis. For the phase purity checking measurement, $0.02^\circ/\text{step}$, $5^\circ/\text{min}$ was used for the θ - 2θ scan. For the lattice constant measurement, the scan speed is reduced to $1^\circ/\text{min}$. From the (001) peak positions, which can be obtained from the computer with the XRD software, we can calculate the lattice constant c . Crystalline quality of the doped films was also examined with an ion channeling technique. Rutherford backscattering spectroscopy (RBS) and energy dispersive spectroscopy were used to measure the composition of the thin films. A standard four-probe technique was used to measure the transport property of these films from room temperature down to liquid-helium temperature. For some samples that had very high resistance ($>10\text{ M}\Omega$), an electrometer was used instead of the four-probe method.

RESULTS AND DISCUSSION

Figure 1 shows the XRD patterns of the $\text{PrBa}_{0.7}\text{Sr}_{1.3}\text{Cu}_3\text{O}_7$ target, $\text{PrBa}_{0.7}\text{Sr}_{1.3}\text{Cu}_3\text{O}_7$ thin film, and PBCO thin film. Obviously, the target contains impurity phases as shown around 32° (2θ) by stars [Fig. 1(a)] because the dopant concentration

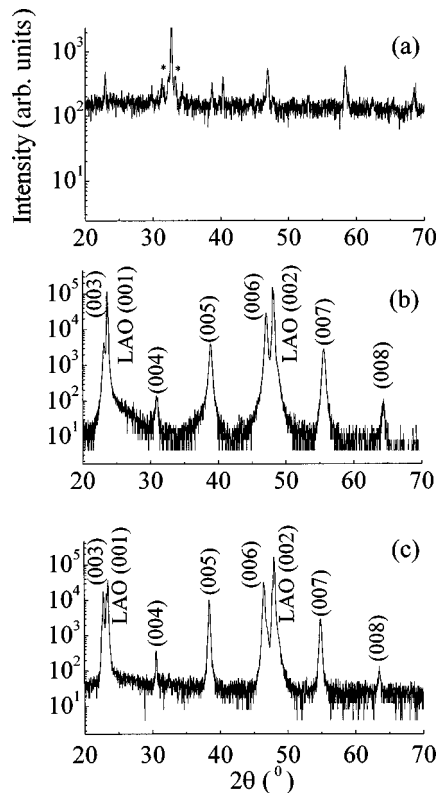


FIG. 1. XRD patterns of (a) the $\text{PrBa}_{0.7}\text{Sr}_{1.3}\text{Cu}_3\text{O}_7$ target (the stars indicate the peaks of impurity phases), (b) a $\text{PrBa}_{0.7}\text{Sr}_{1.3}\text{Cu}_3\text{O}_7$ thin film, and (c) a PBCO thin film. The (001) peaks belong to the 123 phase.

exceeds the solid solubility limit of Sr in PBCO, which is about 0.8.¹⁶ The doped thin films were prepared at 660–780 °C substrate temperatures in 144 mTorr oxygen ambient pressure with a laser energy fluence of 2.8–3.3 J/cm². Under these deposition conditions, all the thin films showed a pure 123 phase. The doped thin film [Fig. 1(b)] shows the pure 123 phase with the *c* axis perpendicular to the surface of the substrate, as can be seen from the XRD pattern of the PBCO thin film [Fig. 1(c)]. For low substrate temperatures (e.g., 660 °C), a *a* axis alignment becomes dominant, i.e., the *a* axis of the doped thin film is perpendicular to the surface of the substrate. Similar results have been obtained in $\text{Pr}_{1-x}\text{Ca}_x\text{Ba}_2\text{Cu}_3\text{O}_7$ thin films grown by PLD.¹⁸

Figure 2 shows the XRD patterns of the $\text{PrBa}_{0.4}\text{Sr}_{1.6}\text{Cu}_3\text{O}_7$ target and thin films. For the target, the amount of the impurity phases increases a lot compared with that of $\text{PrBa}_{0.7}\text{Sr}_{1.3}\text{Cu}_3\text{O}_7$ target, which is understandable on the basis of the increased Sr content. Single phase thin films can be obtained with a substrate temperature of 720–760 °C. Lower substrate temperatures result in the appearance of an impurity phase. In Fig. 2(b), the (003) peak of the thin film merges with the LAO (001) peak. It can be seen that the doped thin film also shows *c* axis alignment.

The (001) peaks of the thin films shift to higher diffraction angles with Sr doping, indicating that the lattice constant along the *c* axis decreases due to Sr doping at Ba sites. The lattice constant *c* is found to be 1.171, 1.165, and 1.159 nm for $\text{PrBa}_{2-x}\text{Sr}_x\text{Cu}_3\text{O}_7$ with $x=0, 1.3,$ and $1.6,$ respectively. The contraction of the lattice constant *c* is consistent with the fact that the ion radius of Sr^{2+} is smaller than that of Ba^{2+} .

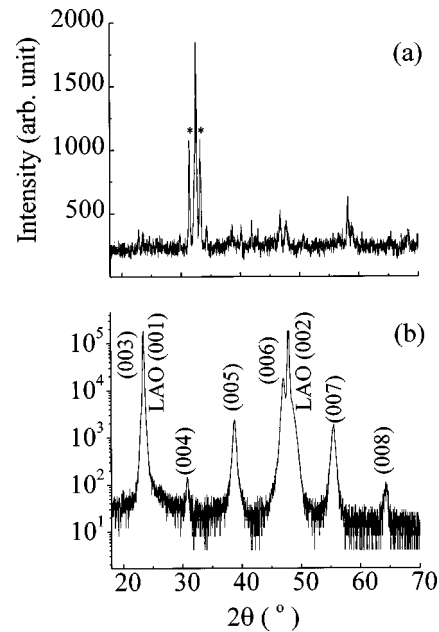


FIG. 2. XRD patterns of the $\text{PrBa}_{0.4}\text{Sr}_{1.6}\text{Cu}_3\text{O}_7$ (a) target and (b) thin film.

For $\text{PrBa}_{2-x}\text{Sr}_x\text{Cu}_3\text{O}_7$ bulk materials, we have shown that the distance between the Pr ions and the oxygen ions in the CuO_2 planes increases, although the lattice constant *c* decreases due to Sr doping.¹⁶ The idea is that when Sr is doped at the Ba site, the nearest neighbor (NN) of Sr will come closer, while the next nearest neighbor (NNN) will come less close to Sr, i.e., the atoms in the unit cell do not move in unison. This results in the increase of the bond length of Pr-O (the CuO_2 plane is the NN of Sr and Pr is the NNN of Sr). Rietveld refinement analysis indeed shows that the Pr-O bond length increases upon Sr doping.¹⁶ Similar results have been obtained in $\text{Tl}(\text{Ba}_{1-x}\text{Sr}_x)_2\text{PrCu}_2\text{O}_7$ (1212 phase) compound,¹⁹ which is an isostructure of $\text{PrBa}_2\text{Cu}_3\text{O}_7$. We believe that this idea can also be applied to the doped thin films. Later it will be shown that the transport results of the doped thin films can be explained using this scenario.

The ϕ scan of the (103) peak of the doped thin films shows four peaks separated by 90°. This fourfold symmetry shows good *a-b* plane alignment indicating epitaxial growth of the thin films. RBS measurements show that the composition of the thin films is consistent with the composition of the targets. Ion channeling measurements on the doped thin films show a 6% minimum yield, which again confirms good crystallinity.

Figure 3 shows the temperature dependence of the resistivity of $\text{PrBa}_{0.7}\text{Sr}_{1.3}\text{Cu}_3\text{O}_7$ thin films with different substrate temperatures. It can be seen that the resistivity of the thin films decreases with the decrease of the substrate temperature, especially low-temperature resistivity, although these thin films all show a pure 123 phase. Similar results were obtained for $\text{PrBa}_{0.4}\text{Sr}_{1.6}\text{Cu}_3\text{O}_7$ thin films, as shown in Fig. 4. These results may be explained by the substrate temperature influence on the desorption of Sr from the substrate during deposition. Energy dispersive x-ray analysis (EDX) measurements show that Sr concentration of the thin films prepared at higher substrate temperatures is a little bit less than those prepared at lower substrate temperatures, thus supporting

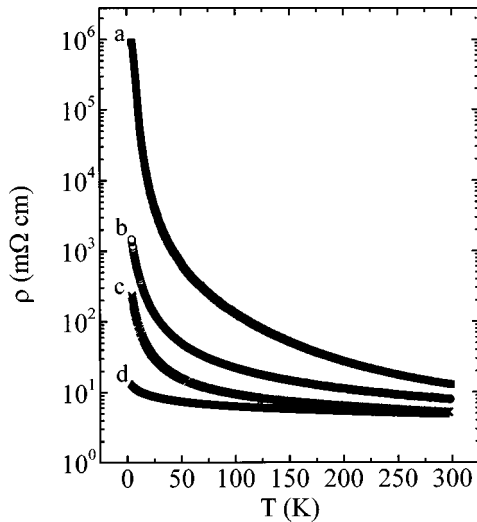


FIG. 3. Temperature dependence of the resistivity of $\text{PrBa}_{0.7}\text{Sr}_{1.3}\text{Cu}_3\text{O}_7$ with different substrate temperatures: (a) 780 °C, (b) 760 °C, (c) 740 °C, and (d) 660 °C.

this explanation. For example, the $\text{PrBa}_{0.7}\text{Sr}_{1.3}\text{Cu}_3\text{O}_7$ thin film prepared at a 780 °C substrate temperature shows a 10% decrease of Sr concentration relative to that of the $\text{PrBa}_{0.7}\text{Sr}_{1.3}\text{Cu}_3\text{O}_7$ thin film prepared at a 660 °C substrate temperature. Furthermore, the lattice constant c is shorter for the doped thin films prepared at a low substrate temperature than that prepared at a high substrate temperature, consistent with the idea that the Sr concentration of the doped thin films increases with decreasing substrate temperature. For example, the lattice constants c are 1.1653 and 1.1621 nm for the $\text{PrBa}_{0.7}\text{Sr}_{1.3}\text{Cu}_3\text{O}_7$ thin films with 780 and 740 °C substrate temperatures, respectively, while the lattice constants c are 1.1588 and 1.1576 nm for the $\text{PrBa}_{0.4}\text{Sr}_{1.6}\text{Cu}_3\text{O}_7$ thin films with 760 and 740 °C substrate temperatures, respectively. So for the thin films prepared at a lower substrate temperature, more Sr was doped into the thin films, resulting in lower resistivity.

Figure 5 shows the temperature dependence of the resis-

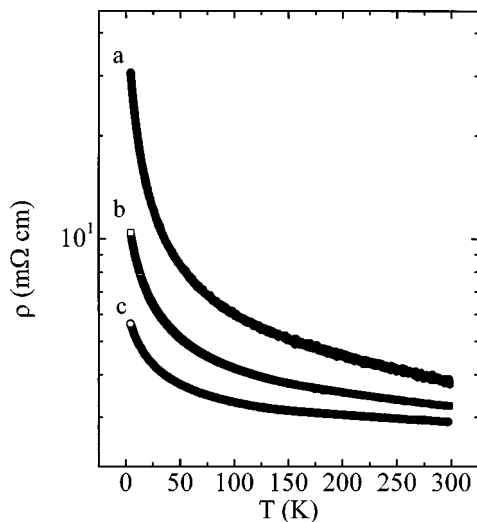


FIG. 4. Temperature dependence of the resistivity of $\text{PrBa}_{0.4}\text{Sr}_{1.6}\text{Cu}_3\text{O}_7$ thin films with different temperatures: (a) 760 °C, (b) 740 °C, and (c) 720 °C.

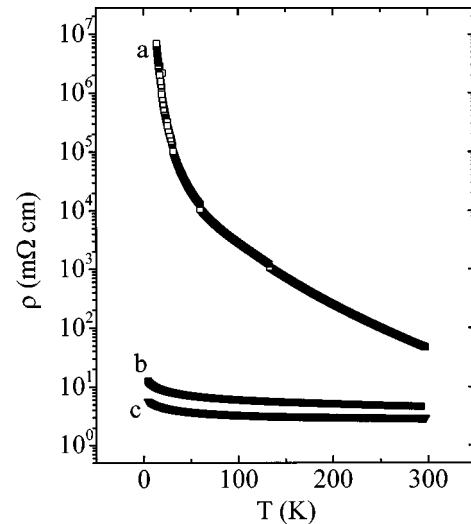


FIG. 5. Temperature dependence of the resistivity for (a) PBCO, (b) $\text{PrBa}_{0.7}\text{Sr}_{1.3}\text{Cu}_3\text{O}_7$, and (c) $\text{PrBa}_{0.4}\text{Sr}_{1.6}\text{Cu}_3\text{O}_7$ thin films.

tivity of PBCO, $\text{PrBa}_{0.7}\text{Sr}_{1.3}\text{Cu}_3\text{O}_7$, and $\text{PrBa}_{0.4}\text{Sr}_{1.6}\text{Cu}_3\text{O}_7$ thin films. It can be seen that Sr doping leads to the decrease of resistivity. This is consistent with the idea that Sr doping increases the distance between Pr and O ions in the CuO_2 plane, leading to the decrease of hybridization between Pr 4*f* and O 2*p* states. Therefore the localization of the holes in the CuO_2 plane becomes weaker and the resistivity of the thin films decreases, especially at low temperatures. It has been found that $\rho(4.2\text{ K})/\rho(300\text{ K})=2.56$ for the $\text{PrBa}_{0.7}\text{Sr}_{1.3}\text{Cu}_3\text{O}_7$ thin film and $\rho(4.2\text{ K})/\rho(300\text{ K})=1.98$ for the $\text{PrBa}_{0.4}\text{Sr}_{1.6}\text{Cu}_3\text{O}_7$ thin film. For the PBCO thin film, $\rho(13\text{ K})/\rho(293\text{ K})=1.27 \times 10^5$. In the $\text{Y}_{1-x}\text{Pr}_x\text{Ba}_2\text{Cu}_3\text{O}_7$ polycrystalline bulk sample, the insulator-metal or superconductor transition occurs around $x=0.45$.²⁰ For $x=0.5$, the electrical resistivity ratio $\rho(4.2\text{ K})/\rho(300\text{ K}) \sim 2.6$. So we can deduce that our $\text{PrBa}_{0.4}\text{Sr}_{1.6}\text{Cu}_3\text{O}_7$ thin film with $\rho(4.2\text{ K})/\rho(300\text{ K})=1.98$ is very close to the insulator-metal transition. It is noticed that room-temperature resistivity of $\text{PrBa}_{0.4}\text{Sr}_{1.6}\text{Cu}_3\text{O}_7$ is around $2.5 \times 10^{-3}\ \Omega\text{ cm}$, which is one order lower than that of the $\text{Y}_{0.5}\text{Pr}_{0.5}\text{Ba}_2\text{Cu}_3\text{O}_7$ polycrystalline bulk material ($1.5 \times 10^{-2}\ \Omega\text{ cm}$).²⁰ For bulk polycrystalline materials, the resistivity contains two parts. One is the intragrain contribution, that is intrinsic, and the other is the intergrain contribution, which is dominated by grain boundaries and thus extrinsic. Generally speaking, the resistivity of the grain boundaries is much higher than that of the bulk for the high- T_c superconductor related materials. This is why the insulator-metal transition resistivities are different for polycrystalline bulk and thin-film samples. The difference between the resistivity of the polycrystalline bulk and thin-film samples for the insulator-metal transition has also been noticed by Infante *et al.*²¹ It has been found that both the composition controlled and temperature induced insulator-metal transitions, shown by the sign of the temperature coefficient of resistivity changing from negative to positive, occurs at the universal value of $2 \times 10^{-3}\ \Omega\text{ cm}$ for oxide thin films.²¹ This is explained quantitatively by Mott's theory of minimum metallic conductivity based on the idea of Anderson localization and the concept of a minimum mean-free path of the order of the distance between atoms (Ioffe-Regel prin-

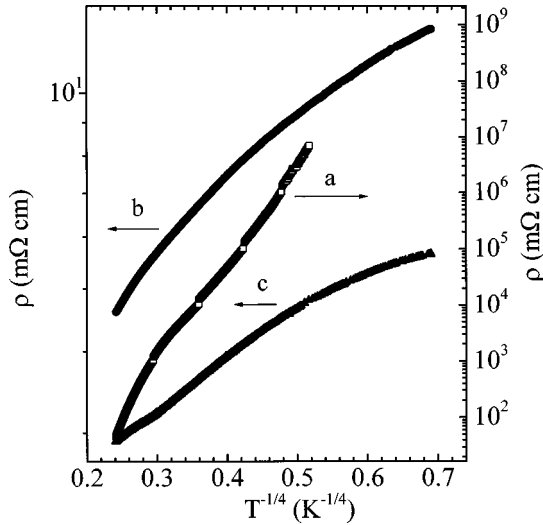


FIG. 6. $T^{-1/4}$ dependence of the resistivity for (a) PBCO, (b) $\text{PrBa}_{0.7}\text{Sr}_{1.3}\text{Cu}_3\text{O}_7$, and (c) $\text{PrBa}_{0.4}\text{Sr}_{1.6}\text{Cu}_3\text{O}_7$ thin films.

ple) in the solid,²² and the Ioffe-Regel limit for resistivity is found to be $2 \times 10^{-3} \Omega \text{ cm}$ that is consistent with the universal value for insulator-metal transitions. It is also shown that the resistivity along the c axis (ρ_c) in high- T_c superconductors shows metallic behavior when its resistivity along the c axis is below the Ioffe-Regel limit, while it shows semiconductorlike behavior when its resistivity along the c axis is above the Ioffe-Regel limit.²³ Again, we can see that the resistivity of the $\text{PrBa}_{0.4}\text{Sr}_{1.6}\text{Cu}_3\text{O}_7$ thin film ($2.5 \times 10^{-3} \Omega \text{ cm}$) is very close to the Ioffe-Regel limit. For the $\text{Y}_{1-x}\text{Pr}_x\text{Ba}_2\text{Cu}_3\text{O}_7$ single crystal, the insulator-metal transition occurs around $x=0.55$ with a resistivity of $2.5 \times 10^{-3} \Omega \text{ cm}$,²⁴ which is comparable to the resistivity of the $\text{PrBa}_{0.4}\text{Sr}_{1.6}\text{Cu}_3\text{O}_7$ thin film. It has been shown in our previous paper that the strain effect caused by the lattice mismatch between the thin film and substrate also affects the electrical transport property of the doped thin films.²⁵ So, if a suitable substrate is used, it will favor the insulator-metal transition. In fact, we have prepared some $\text{PrSr}_2\text{Cu}_3\text{O}_7$ thin films. Although the phase of the thin films is not very pure, some samples showed metallic behavior above 100 K, which is very interesting and worth further study. It should be mentioned that the hybridization between the Pr $4f$ and O $2p$ states increases with decreasing temperature if we consider that the distance between the Pr ions and oxygen ions decreases with decreasing temperature. This will contribute to the temperature dependence of the resistivity and other properties. The temperature dependence of the resistivity for some $\text{PrSr}_2\text{Cu}_3\text{O}_7$ thin films may be explained on the basis that the hybridization between Pr $4f$ and O $2p$ states is very weak above 100 K and increases below 100 K due to the contraction of the unit cell with decreasing temperature, resulting in the resistivity increase at lower temperatures.

In Fig. 6, we used the three-dimensional (3D) VRH conductivity model to fit the transport data. For the 3D VRH mechanism, $\rho(T) = \rho_0 \exp(T_0/T)^{1/4}$, and $T_0 = \beta/[k_B N(0)d^3]$, where $N(0)$ is the density of states at the Fermi level, d is the localization radius of the states near the Fermi level, k_B is the Boltzmann's constant, and β is a numerical coefficient. The resistivity of PBCO can be fitted

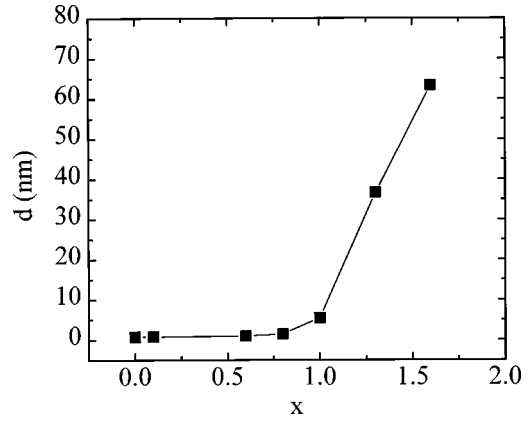


FIG. 7. Variation of the localization radius d with Sr doping for the $\text{PrBa}_{2-x}\text{Sr}_x\text{Cu}_3\text{O}_7$ samples.

from 100 K to lower temperatures, which is consistent with the published results.⁴ However, in the case of doped thin films, the resistivity cannot be fitted well, which may be due to the dramatic decrease of the localization of the carriers. If we assume that the resistivity of the doped thin films is still dominated by VRH at low temperatures, we can obtain the value of T_0 by using the curves at lower temperatures given in Fig. 6. Then, using the values $N(0) = 10^{21}/\text{cm}^3 \text{ eV}$, $\beta = 20$,³ and assuming that $N(0)$ does not change with doping, we can obtain the localized radius, d . The dependence of d on the doping is shown in Fig. 7. Data from previous work is also shown in the figure.¹⁶ It can be seen that the localization length is greatly increased at a higher doping level. This can be explained by the decrease of the hybridization between Pr $4f$ and O $2p$ states due to Sr doping. It should be mentioned that the strain effect that originated from the lattice constant mismatch between the doped thin films and the LAO substrate also contribute to the decrease of the hybridization because this strain effect increases the distance between Pr ions and oxygen ions in the CuO_2 planes.²⁵

For the PBCO thin films, we found that an impurity phase

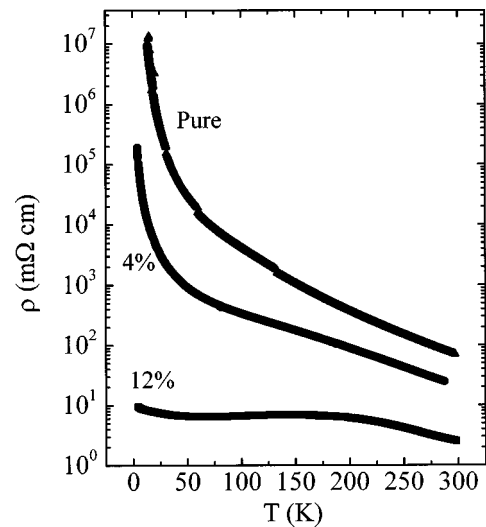


FIG. 8. Temperature dependence of the resistivity for PBCO thin films with a different amount of the impurity phase. The percentage in the figure corresponds to the intensity ratio of the 42° peak relative to that of the PBCO (005) peak.

peak at around 42° (2θ), which may be related to BaCuO_2 , has a dramatic influence on the temperature dependence of the resistivity. The increase of this peak intensity is accompanied by a large resistivity drop at low temperatures, relative to that of the pure phase PBCO thin films. Figure 8 shows the temperature dependence of the resistivity for PBCO thin films with different amounts of the impurity phase. It should be pointed out that the curve for the PBCO with a 12% impurity phase is similar to some paper about the temperature dependence of the resistivity of PBCO thin films.²⁶ So the impurity phase has a dramatic effect on the resistivity of PBCO thin films. It is possible that the resistivity of the impurity phase is lower compared with that of the pure PBCO phase, leading to percolation paths in the thin films. An alternative is that the existence of the impurity phase results in some vacancies in the PBCO phase. These vacancies produce distortion in the PBCO structure or delocalization of the carriers.

Recently, Zou *et al.* found that the PBCO single crystals prepared by the travelling-solvent floating-zone (TSFZ) technique show bulk superconductivity with T_c around 80 K after annealing in oxygen atmosphere, while PBCO single crystals prepared by the slow cooling technique remain semiconducting.² One remarkable difference is that the c

axis for TSFZ PBCO single crystals is longer than that of PBCO crystals prepared by other techniques. This may indicate that the hybridization between Pr $4f$ and O $2p$ states is rendered very weak due to the lattice constant c increase in the TSFZ PBCO single crystals, which then leads to the recovery of superconductivity.

In summary, we have prepared single phase epitaxial $\text{PrBa}_{2-x}\text{Sr}_x\text{Cu}_3\text{O}_7$ ($x=0,1.3,1.6$) thin films by PLD with the dopant concentration far exceeding the solid solubility limit. The resistivity of the doped thin films dramatically decreases, which can be explained by the Sr doping induced decrease of the hybridization between the Pr $4f$ and O $2p$ states. The $\text{PrBa}_{0.4}\text{Sr}_{1.6}\text{Cu}_3\text{O}_7$ thin film is very close to the insulator-metal transition and, with further doping or induced strain from an appropriate substrate, the sample could be made metallic or even superconducting.

ACKNOWLEDGMENTS

We would like to thank R. L. Greene, S. B. Ogale, S. P. Pai, Z. Y. Chen, and R. Shreekala for valuable discussions and help in this work. This work was supported by NSF Grant No. DMR9404579 and the NSF MRSEC program at the University of Maryland.

*On leave from the Department of Physics, Tsinghua University, Beijing 100084, China; Electronic address: yzhao@squid.umd.edu

[†]Also at Materials Research Science and Engineering Center, University of Maryland.

¹For a review, see, H. B. Radousky, Mater. Res. Bull. **7**, 1917 (1992).

²Zhigang Zou, Kunihiro Oka, Toshimitsu Ito, and Yoshikazu Nishihara, Jpn. J. Appl. Phys., Part 2 **36**, L18 (1997).

³Yunhui Xu and Weiyan Guan, Physica C **206**, 59 (1993).

⁴B. Fisher, J. Genossar, L. Patlagan, G. M. Reisner, C. K. Subramaniam, and A. B. Kaiser, Phys. Rev. B **50**, 4118 (1994).

⁵A. Kebede, C. S. Jee, J. Schwegler, J. E. Crow, T. Mihalisin, G. H. Myer, R. E. Salomon, P. Schlottmann, M. V. Kuric, S. H. Bloom, and R. P. Guertin, Phys. Rev. B **40**, 4453 (1989).

⁶I. Felner, U. Yaron, I. Nowik, E. B. Bauminger, Y. Wolfus, E. R. Yacoby, G. Hilscher, and N. Pillmayr, Phys. Rev. B **40**, 6739 (1989).

⁷J. S. Kang, J. W. Allen, Z. X. Shen, W. P. Ellis, J. J. Yeh, B. W. Lee, M. B. Maple, W. E. Spicer, and I. Lindau, J. Less-Common Met. **148**, 121 (1989).

⁸G. Y. Guo and W. M. Temmerman, Phys. Rev. B **41**, 6372 (1990).

⁹L. Soderholm and G. L. Goodman, J. Solid State Chem. **81**, 121 (1989).

¹⁰A. P. Goncalves, I. C. Santos, E. B. Lopes, R. T. Henriques, M. Almeida, and M. O. Figueiredo, Phys. Rev. B **37**, 7476 (1988).

¹¹J. J. Neumeier, M. B. Maple, and M. S. Torikachvili, Physica C **156**, 574 (1988).

¹²G. L. Goodman, C. K. Loong, and L. Soderholm, J. Phys.: Condens. Matter **3**, 49 (1991); G. L. Goodman and L. Soderholm, Physica C **171**, 528 (1990).

¹³X. X. Tang, A. Manthiram, and J. B. Goodenough, Physica C **161**, 574 (1989).

¹⁴L. Soderholm, C. K. Loong, G. L. Goodman, U. Welp, J. Bolender, and C. W. Williams, Physica B **163**, 655 (1990).

¹⁵J. B. Torrance and R. M. Metzger, Phys. Rev. Lett. **63**, 1515 (1989).

¹⁶Y. G. Zhao, S. Y. Xiong, Y. P. Li, B. Zhang, S. S. Fan, B. Yin, J. W. Li, S. Q. Guo, W. H. Tang, G. H. Rao, D. J. Dong, B. S. Cao, and B. L. Gu, Phys. Rev. B **56**, 9153 (1997).

¹⁷C. R. Fincher and G. B. Blanchet, Phys. Rev. Lett. **67**, 2902 (1991).

¹⁸D. P. Norton, D. H. Lowndes, B. C. Sales, J. D. Budai, B. C. Chakoumakos, and H. R. Kerchner, Phys. Rev. Lett. **66**, 1537 (1991); D. P. Norton, D. H. Lowndes, B. C. Sales, J. D. Budai, E. C. Jones, and B. C. Chakoumakos, Phys. Rev. B **49**, 4182 (1994).

¹⁹C. C. Lai, T. J. Lee, H. K. Fun, H. C. Ku, and J. C. Ho, Phys. Rev. B **50**, 4092 (1994).

²⁰J. L. Peng, P. Klavins, R. N. Shelton, H. B. Radousky, P. A. Hahn, and L. Bernardez, Phys. Rev. B **40**, 4517 (1989).

²¹C. Infante, M. K. El Mously, R. Dayal, M. Husain, S. A. Siddiqi, and P. Ganguly, Physica C **167**, 640 (1990).

²²N. F. Mott, Adv. Phys. **16**, 49 (1967); Philos. Mag. B **44**, 265 (1981); N. F. Mott and M. Kaveh, Adv. Phys. **34**, 329 (1985); N. F. Mott, *Metal-Insulator Transitions* (Taylor & Francis, London, 1990).

²³T. Ito, H. Takagi, S. Ishibashi, T. Ido, and S. Uchida, Nature (London) **350**, 596 (1991).

²⁴Wu Jiang, Ph.D. thesis, University of Maryland, 1993.

²⁵Y. G. Zhao, Z. W. Dong, M. Rajeswari, R. P. Sharma, and T. Venkatesan, Appl. Phys. Lett. **72**, 981 (1998).

²⁶H. Iwasaki, S. Kenmochi, O. Taniguchi, and N. Kobayashi, Physica C **204**, 406 (1993).